Quantum Field Theory of Nematic Transitions in Spin-Orbit-Coupled Spin-1 Polar Bosons

E. J. König and J. H. Pixley

Department of Physics and Astronomy, Center for Materials Theory, Rutgers University, Piscataway, New Jersey 08854, USA

We theoretically study an ultracold gas of spin-1 polar bosons in a one-dimensional continuum, which are subject to linear and quadratic Zeeman fields and a Raman induced spin orbit coupling. Concentrating on the regime in which the background fields can be treated perturbatively, we analytically solve the model in its low-energy sector; i.e., we characterize the relevant phases and the quantum phase transitions between them. Depending on the sign of the effective quadratic Zeeman field ϵ, two superfluid phases with distinct nematic order appear. In addition, we uncover a spin-disordered superfluid phase at strong coupling. We employ a combination of renormalization group calculations and duality transformations to access the nature of the phase transitions. At $\epsilon = 0$, a line of spin-charge separated pairs of Luttinger liquids divides the two nematic phases, and the transition to the spin-disordered state at strong coupling is of the Berezinskii-Kosterlitz-Thouless type. In contrast, at $\epsilon \neq 0$, the quantum critical theory separating nematic and strong coupling spin-disordered phases contains a Luttinger liquid in the charge sector that is coupled to a Majorana fermion in the spin sector (i.e., the critical theory at finite ϵ maps to a quantum critical Ising model that is coupled to the charge Luttinger liquid). Because of an emergent Lorentz symmetry, both have the same logarithmically diverging velocity. We discuss the experimental signatures of our findings that are relevant to ongoing experiments in ultracold atomic gases of ^{23}Na.

The interplay of internal quantum states and strong interactions can lead to the emergence of new quantum phases of matter and criticality. For example, while spin-1/2 quantum magnets can only sustain conventional magnetic order, larger spin systems allow for order in higher angular momentum channels involving multipole moments in large spin systems [1–3]. Spinful ultracold atomic gases are a particularly fruitful setting to study magnetic phenomena with spins $S > 1/2$, where optical traps allow for the cooling and manipulation of all of the internal hyperfine states of the atom, thus realizing atomic gases with a large spin (e.g., ^{52}Cr with $S = 3$) [4,5]. This can lead to superfluids with non-trivial magnetic structure that spontaneously break both charge conservation and spin rotation symmetries [6,7].

Ultracold spin-1 bosons are an ideal system to study nontrivial magnetism beyond conventional vector magnetic order parameters. A pivotal microscopic ingredient is the spin dependent interaction g_2, which can either be ferromagnetic ($g_2 < 0$) or polar ($g_2 > 0$) [5] and leads to different ground states displaying either nonzero or zero spin expectation value, respectively [6,7]. In the following, we concentrate on the polar case, which is readily realized with ^{23}Na gases [5]. The condensate wave function can be written as a three-component spinor $\Psi_{MF} = \sqrt{\rho} e^{i\vartheta} \hat{n}$, where the superfluid phase ϑ and the unit vector $\hat{n}$ parametrize the ground state manifold. The polar condensate has nematic order signaled by nonzero eigenvalues of a rank-2 tensor

order parameter [6,7]. A quadratic Zeeman field [8] lifts the degeneracy, and the ground state spinor is given by either $\hat{n} = (0, 1, 0)^T$ or a planar state $\hat{n} = (e^{i\varphi}, 0, e^{-i\varphi})^T$, depending on the sign of the quadratic Zeeman field [4]. In recent
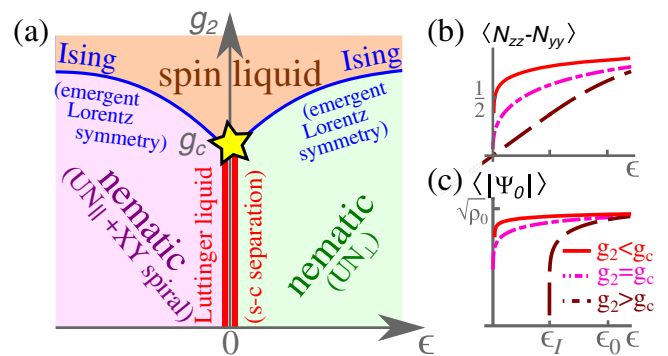

FIG. 1. (a) Phase diagram in the plane spanned by effective quadratic Zeeman field $\epsilon = q + \Theta^2/(2m)$ and spin-spin interaction g_2. For explanations on the two nematic phases and the spin liquid, see the main text. The nonuniversal position g_c of the BKT transition is marked by a star. (b) Difference of the only nonzero nematicity tensor components $\langle N_{zz} - N_{yy} \rangle$; note that it is odd in ϵ and $\langle N_{yy} + N_{zz} \rangle = 1$. The characteristic power law is nonuniversal $|\epsilon|^{1/(2K_s-1)}$, $K_s \geq 2$ for $g_2 \leq g_c$, and linear for $g_2 > g_c$. (c) The $m_z = 0$ component of the Bose-Einstein condensate wave function (the order parameter) scales as $\epsilon^{(1/4)/(2K_s-1)}$ for $g_2 \leq g_c$ and $(\epsilon - \epsilon_I)^{1/8}$ for $g_2 > g_c$.

experiments, it has been demonstrated that it is possible to observe the nontrivial nematic order in ^{23}Na [9] and that the quadratic Zeeman effect can be used to drive nematic phase transitions [10,11]. Moreover, the nematic planar phase is interesting due to the different types of topological defects that can result from the winding of the phase $\vartheta \to \vartheta + 2\pi$ or the combined operation of a *half*-winding of the phase $\vartheta \to \vartheta + \pi$ and an inversion of the spinor $\hat{n} \to -\hat{n}$ that leave Ψ_{MF} unchanged [12–14], which have recently been observed in ^{23}Na [15].

With the latest development of artificial gauge fields, it is now possible to couple the internal spin states of the atom to their momentum using counterpropagating Raman lasers, which induces an effective spin orbit coupling (SOC) [16]. Spin orbit coupled quantum gases can now be realized in spinor bosons [17–21] or spinful fermions [22] with either a one- or two-dimensional SOC [23–26]. In bosonic gases, this gives rise to "striped" superfluids [27–36] that condense at the degenerate momenta dictated by the spin orbit wave vector. While the phase diagram is now reasonably well understood, spin orbit coupled, polar, spin-1 gases offer an exciting platform to study the competition between different types of nematic order and hold great promise for intriguing forms of quantum criticality. A majority of the theoretical [28,32–35,37,38] and experimental [17–21] work has focused on quantum phase transitions (QPTs) that are driven by the strength of the Raman field and are accessible in both pseudospin-1/2 and spin-1 bosons. Interestingly, for polar spin-1 bosons, the phenomena and nematic QPTs that can be evoked by SOC goes beyond transverse field induced transitions and remains largely unexplored apart from mean field (MF) [35,39] and variational solutions [33,36,40]. Our work aims to fill this gap by developing a field theory description of nematic QPTs.

One major difficulty in theoretically capturing the interplay between nonperturbative topological defects, SOC, and nematic order is that it requires a strong coupling solution beyond any MF-like description. Thus, one of the most felicitous realms to study spin orbit coupled polar spinor bosons are one-dimensional (1D) systems, which represent a common setup for ultracold atom experiments. This is due to the existence of strong analytical tools that allow for asymptotically exact low-energy solutions that take into account both the inherent strong coupling nature of 1D and topological defects [41–43]. The effective field theory of polar spin-1 bosons in the absence of a SOC is described by a spin-charge separated Lagrangian, the charge is described by a gapless Luttinger liquid (LL), and the spin sector is given by a 1D nonlinear sigma model (NLσM) [41,43]. A SOC directly couples the spin and charge degrees of freedom and therefore it is in no way obvious if spin-charge separation can still persist in spin orbit coupled gases.

Summary of results and experimental predictions.—We consider a gas of 1D polar spinor bosons in the presence of a SOC (wave vector Θ) and a linear (quadratic) Zeeman field hp (q). We treat the strength of background fields perturbatively and derive the effective low-energy field theory that describes a LL coupled to a NLσM in the presence of anisotropic mass terms. We solve this effective theory in the low-energy limit and determine the phase diagram of the model (see Fig. 1). We uncover three distinct superfluid phases: at weak coupling, two different nematic phases, depending on the sign of the effective quadratic Zeeman field $\epsilon = q + \Theta^2/(2m)$, and a spin liquid phase at strong coupling. Furthermore, we determine the nature of the QPTs between those phases, all of which are continuous. The critical state between the two nematic phases at weak coupling is a pair of spin-charge separated Luttinger liquids. In contrast, the transition from either nematic phase to the spin liquid is in the $1 + 1$D Ising universality class, with an exotic, emergent Lorentz symmetry characterized by equal, logarithmically divergent velocities in the spin and charge sector. Interestingly, a very similar QPT was discussed in the physically unrelated context of Cooper pairing near Lifshitz transitions and in topological superconductors [44–46]. Finally, Ising and LL QPT lines meet at a Berezinskii-Kosterlitz-Thouless (BKT) critical point.

The hallmarks of our theory are as follows. (i) The described phases and fluctuation induced continuous QPTs. We emphasize that MF and variational theories predict a first order transition at $\epsilon = 0$ and miss the spin liquid phase completely. (ii) The order parameter of the QPTs are the spin components of the condensate wave function [see Fig. 1(c)]. (iii) An experimentally accessible observable is the nematic tensor $N_{ab} = \delta_{ab} - \{S_a, S_b\}/2$ [see Fig. 1(b)]. We predict a characteristic power law behavior of N_{yy}, N_{zz} with nonuniversal exponents. This emblematic feature of LL physics is out of reach of MF theory. For parameters in typical ultracold atom experiments with quasi-1D tubes of atoms at nano-Kelvin temperatures, we estimate $K_s \sim O(10)$ and a system size and thermal length that exceed the correlation length (see Supplemental Material [47]). Thus, these power laws should be experimentally detectable. (iv) The effect of SOC is twofold: First, the condensate wave function in the nematic $\epsilon < 0$ phase is heavily modulating in space. Second, SOC strongly affects the position of QPTs. However, somewhat strikingly, the universal critical behaviors are independent of the SOC. (v) Finally, the emergent Lorentz symmetry at the Ising transitions is, at least in principle, accessible via separate measurement of excitation spectra in charge and spin sectors [48,49]. In the remainder, we present the theoretical framework leading to these results and predictions.

Model.—Continuum spin-1 bosons with mass m that are perturbed by a background helical magnetization and a constant linear Zeeman field $\vec{h}(x) = h(\cos(\Theta x), -\sin(\Theta x), p)^T$, as well as a quadratic Zeeman coupling q, can be described by the normal ordered Hamiltonian density $\mathcal{H} = \partial_x \Psi^\dagger \partial_x \Psi/(2m) + \mathcal{H}_2 + \mathcal{H}_4$, where

$$\mathcal{H}_2 = q\Psi^\dagger S_z^2 \Psi + \Psi^\dagger \vec{h}(x) \cdot \vec{S}\Psi, \tag{1a}$$

$$\mathcal{H}_4 = \frac{g_0}{2} : (\Psi^\dagger \Psi)^2 : + \frac{g_2}{2} : (\Psi^\dagger \vec{S}\Psi)^2 :. \tag{1b}$$

We analyze the polar case $g_0 > g_2 > 0$ ($g_0 \sim 32 g_2$ in ^{23}Na [5]) in the semiclassical limit, in which the condensate density $\rho_0 = \mu/g_0$ parametrically exceeds the inverse coherence length $1/\xi_c = \sqrt{2m\mu}$. Here, μ is the chemical potential and we set $\hbar = k_B = 1$ throughout.

The bosonic field operators Ψ, $\Psi^\dagger$ are three component spinors, and in the remainder, we choose the adjoint representation of **SU**(2) as a basis of spin-1 operators $(S_a)_{bc} = -i\epsilon_{abc}$, with $a, b, c \in \{x, y, z\}$. The quartic term can be recast into the form $\mathcal{H}_4 = (g_0 + g_2)/2 : (\Psi^\dagger \Psi)^2 : -g_2/2 : [\Psi^\dagger \Psi^*][\Psi^T \Psi]:$ so that the $[\mathbf{U}(1) \times \mathbf{O}(3)]/\mathbb{Z}_2$ symmetry of the unperturbed action becomes manifest. Equation (1) describes the quantum fluid in the lab frame, the frame corotating with the Raman field can be accessed by $\Psi \to e^{i\Theta x S_z}\Psi$. In this frame, Eq. (1) retains its structure, except for $\vec{h} \to h(1, 0, p)^T$ and $\partial_x \to \partial_x + i\Theta S_z$ (this yields $q \to \epsilon = q + \Theta^2/2m$).

In order to solve Eq. (1) in its low-energy sector, we perform a sequence of coarse graining steps, which are motivated by the assumption of the hierarchy of length scales presented in Fig. 2. The meaning of each of those scales will be explained at the appropriate position of the main text. Since the dispersion relation of collective modes is linear [see Eq. (2) below], the conversion to equivalent time (energy) scales follows trivially.

Effective low-energy theory.—As a first step towards the asymptotic solution of Eq. (1), we derive the effective long-wavelength Matsubara field theory [41,43] (for details, see Supplemental Material [47]). It is convenient to choose an Euler angle parametrization $\Psi = \sqrt{\rho}e^{i\vartheta}Oe^{i\alpha_4\lambda_4}e^{i\alpha_6\lambda_6}\hat{e}_z$, with λ_i being Gell-Mann matrices. This representation separates the Goldstone modes $e^{i\vartheta}$, $O = e^{i\alpha_7\lambda_7}e^{i\alpha_5\lambda_5}$ living on the manifold $[\mathbf{U}(1) \times \mathbf{O}(3)/\mathbf{O}(2)]/\mathbb{Z}_2$ from the massive longitudinal modes α_4 and α_6 from the outset. This representation of the complex unit vector $\Psi/\sqrt{\rho}$ provides a regular Jacobian leading to the NLσM measure for the Goldstone field $\hat{n} \equiv O\hat{e}_z \in \mathbb{S}^2$. While constant ϑ and O
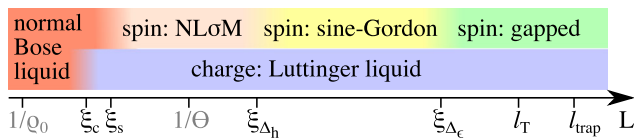

FIG. 2. Length scales of the problem away from criticality. The large superfluid density and the slow SOC pitch $\rho_0 \gg 1/\xi_{c,s} \gg \Theta$ enable the controlled derivation of Eq. (2). The perturbative inclusion of the effective fields $|\epsilon|$, $h \ll \mu$, implies $\xi_{c,s} \ll \xi_{\Delta_h} < \xi_{\Delta_\epsilon}$ (the last inequality reflects the focus on SOC). At each length scale $\xi_{c,s,\Delta_h,\Delta_\epsilon}$, certain modes freeze and an effective theory emerges.

fields are zero modes of $\mathcal{H} - \mathcal{H}_2$, Eqs. (1a) and (1b) ensure that the longitudinal modes take the saddle point values $\rho_{\text{MF}} = \rho_0 - q\hat{n}S_z^2\hat{n}/g_0$, $\alpha_{4,\text{MF}} = -i\hat{e}_z^T O^T\vec{h} \cdot \vec{S}O\hat{e}_x/[2\rho_0 g_2]$, and $\alpha_{6,\text{MF}} = -i\hat{e}_z^T O^T\vec{h} \cdot \vec{S}O\hat{e}_y/[2\rho_0 g_2]$, which are perturbative in $hg_0/(\mu g_2)$ but nonperturbative in q. Fluctuations around the saddle point $\Delta\rho$ ($\Delta\alpha_{4,6}$) decay on the length scale ξ_c ($\xi_s = \sqrt{g_0/g_2}\xi_c$). To access the physics at longer scales, we perform the Gaussian integration of massive modes, assuming that O and ϑ are slow. We switch to the corotating frame and obtain the effective low-energy Lagrangian $\mathcal{L} = \mathcal{L}_0 + \mathcal{L}_1 + \mathcal{L}_2$,

$$\mathcal{L}_0 = \Delta_\epsilon \hat{n}S_z^2\hat{n} - \Delta_h \hat{n}(S_x + pS_z)^2\hat{n}, \tag{2a}$$

$$\mathcal{L}_1 = -i\dot{\vartheta}\lambda_\epsilon \hat{n}S_z^2\hat{n} + \lambda_h\dot{\hat{n}}S_x\hat{n} + i\lambda_\Theta\hat{n}'S_z\hat{n}, \tag{2b}$$

$$\mathcal{L}_2 = \frac{K_c}{2\pi v_c}[\dot{\vartheta}^2 + v_c^2\vartheta'^2] + \frac{K_s}{2\pi v_s}[|\dot{\hat{n}}|^2 + v_s^2|\hat{n}'|^2]. \tag{2c}$$

The kinetic part of the action [Eq. (2c)], which we denote as $\mathcal{L}_2 = \mathcal{L}_{\text{LL}}[\vartheta] + \mathcal{L}_{\text{NL}\sigma\text{M}}[\hat{n}]$, contains bare coupling constants $K_{c,s} = \sqrt{2}\pi\rho_0\xi_{c,s}$ and velocities $v_c = \sqrt{\rho_0 g_0/m}$ and $v_s = \sqrt{\rho_0 g_2/m}$. We omitted anisotropic corrections to kinetic terms due to q, Θ, and h, because they are small and will renormalize to zero quickly. In addition to the known kinetic term $\mathcal{L}_2$, Eq. (2) contains symmetry breaking terms with no derivatives $\Delta_\epsilon = \rho_0\epsilon$, $\Delta_h = h^2/2g_2$ and one derivative $\lambda_\epsilon = \epsilon/g_0$, $\lambda_h = h/g_2$, $\lambda_\Theta = \Theta\rho_0/m$, which are the focus of this Letter. In the Supplemental Material [47], we treat a weak trapping frequency $\omega_\parallel \ll mg_0^2$ via the replacement $\rho_0 \to \rho_0[1 - x^2/l_{\text{trap}}^2]$. We find that this introduces the largest finite length scale ($l_{\text{trap}} = \sqrt{2\mu/m\omega_\parallel^2}$) into the problem, which is less restrictive then the presence of finite temperature ($l_T = v_s/T$), and their combined effect rounds out the observable critical properties (see Fig. 2).

Characterization of phases.—We begin the asymptotic solution of Eq. (2) by determining all phases and their characteristics [see Fig. 1(a)]. Ground states that are also accessible to variational [33,36,40] and MF [35,39] treatments follow from the consideration of the potential term $\Delta_\epsilon S_z^2 - \Delta_h(S_x + pS_z)^2$, which independently of p predicts a first order transition at $\epsilon = 0$ [47]. For $p = 0$, it has eigenvalues Δ_ϵ, $\Delta_\epsilon - \Delta_h$, $-\Delta_h$ with eigenstates $\hat{e}_x$, $\hat{e}_y$, $\hat{e}_z$, respectively (for $p \neq 0$, see Supplemental Material [47]). At finite h, the ground state at $\epsilon > 0$ ($\epsilon < 0$) is $\Psi_{\text{MF}} \simeq \sqrt{\rho_0}e^{i\vartheta}[\hat{e}_z + h\hat{e}_y/(2g_2\rho_0)]$ ($\Psi_{\text{MF}} \simeq \sqrt{\rho_{\text{MF}}}e^{i\vartheta}[\hat{e}_y - h\hat{e}_z/(2g_2\rho_0)]$), where the finite h corrections stem from $\alpha_{4,6}^{\text{MF}}$. This state is denoted $UN_\perp$ ($UN_\parallel + XY$ spiral) because at MF level it displays uniaxial nematic order $\langle N_{zz} \rangle = \rho_0 + \mathcal{O}(h^2)$ [$\langle N_{yy} \rangle = \rho_0 + \mathcal{O}(h^2)$]. Both states show weak magnetization $\langle S_x \rangle = -h/g_2$. In the lab frame, the

magnetization follows the helical magnetic field and, for $\epsilon < 0$, there is a strong modulation of the superfluid wave function because bosons condense at finite momentum $k = \Theta$, producing a stripe superfluid [47]. MF theory predicts a first order transition at $\epsilon = 0$: the ground state in the spin sector becomes degenerate and the order parameter $\langle N_{ab} \rangle$ changes discontinuously. Finally, there is a third phase in which the spin sector is quantum disordered, i.e., a spin liquid [43]. This occurs when $K_s \to 0$, a scenario that is not captured by the bare parameters entering Eq. (2) but can be reached upon RG transformations.

Characterization of phase transitions.—Having identified the three phases of the problem, we now characterize the nature of the QPTs between them. We first discuss the RG flow close to the repulsive fixed point $K_s = \infty$ at small $\Delta_{\epsilon,h}, \lambda_{\epsilon,h,\Theta}$. It is well known that $dK_s/db = -1/2 + \mathcal{O}(1/K_s, \Delta_{\epsilon,h}, \lambda_{\epsilon,h,\Theta})$. As usual, b denotes the running logarithmic scale. The unperturbed weak coupling theory suggests that the spin liquid is approached at the length scale $\xi_{\text{SL}} \sim \xi_s \exp(\sqrt{2}\pi\rho_0\xi_s)$. However, the scaling dimensions of $\Delta_{\epsilon,h}, \lambda_\epsilon$, and $\lambda_{h,\Theta}$ are $[2 - 3/(2K_s)]$, $[1 - 3/(2K_s)]$, and $[1 - 1/(2K_s)]$, i.e., RG relevant at weak coupling. We define the length scales $\xi_{\Delta_{\epsilon,h}}$ self-consistently as the scale when the couplings $\Delta_{\epsilon,h}(b)$ hit the running scale, by assumption $\xi_{\Delta_h} < \xi_{\Delta_\epsilon}$. Beyond ξ_{Δ_h} the NLσM field is locked to the easy plane $\hat{n} = (0, \sin(\phi), \cos(\phi))^T$ perpendicular to the background magnetization realizing a spin-floplike phase of itinerant polar bosons. Following Fig. 2, a sine-Gordon theory emerges. The coupling to the charge Luttinger liquid is characterized by $\mathcal{L}_{\text{EP}} = \mathcal{L}_{\text{LL}}[\vartheta] + \tilde{\mathcal{L}}$,

$$\tilde{\mathcal{L}} = \frac{K_s}{2\pi v_s}[(\dot{\phi})^2 + v_s^2(\phi')^2] + [\Delta_\epsilon - i\dot{\vartheta}\lambda_\epsilon]\sin^2(\phi). \quad (3)$$

All coupling constants in Eq. (3) are evaluated at the scale ξ_{Δ_h} and we absorbed a factor of $1/(1 + p^2)$ into $\Delta_\epsilon, \lambda_\epsilon$. Note that, while $K_c \gg 1$ by assumption, K_s is large only if $\xi_{\Delta_h} \ll \xi_{\text{SL}}$ and may be renormalized to values of the order of unity or even smaller otherwise. In terms of Eq. (3), the phase $UN_\perp$ ($UN_\parallel + XY$ spiral) is characterized by $\langle \phi \rangle = 0 \mod \pi$ ($\langle \phi \rangle = \pi/2 \mod \pi$).

The fields entering Eq. (3) allow for various topological defects: 2π phase slips in ϑ and ϕ fields as well as π phase slips in ϑ accompanied with a $\pm\pi$ phase slip in ϕ [12]. The scaling dimensions [13,47,50] of the associated fugacities (Boltzmann weights) are $(2 - K_c)$, $(2 - K_s)$, and $[2 - (K_c + K_s)/4]$, respectively. Therefore, in the given parameter regime ($K_c \gg 1$), only the fugacity y of 2π phase slips in the spin field ϕ may be relevant. We incorporate the associated operator into Eq. (3) and derive [47] the weak coupling RG equations to second order in λ_ϵ, Δ_ϵ, y and to zeroth order in $1/K_c$, extending the previously reported [51] results to the case of finite λ_ϵ,

$$\frac{d\Delta_\epsilon}{db} = (2 - 1/K_s)\Delta_\epsilon, \qquad \frac{dy}{db} = (2 - K_s)y,$$

$$\frac{dK_s}{db} = \Delta_\epsilon^2 - K_s^2 y^2, \qquad \frac{d\lambda_\epsilon}{db} = (1 - 1/K_s)\lambda_\epsilon,$$

$$\frac{d(K_c/v_c)}{db} = \frac{\lambda_\epsilon^2}{K_s v_s}, \qquad \frac{d(K_c v_c)}{db} = \frac{dv_s}{db} = 0. \quad (4)$$

Regularization dependent factors were absorbed into a redefinition of λ_ϵ, Δ_ϵ, y. Figure 3(a) displays the RG flow in the plane $(\Delta_\epsilon/y, K_s)$ and illustrates that (i) the MF first order transition at $\epsilon = 0$ for $K_s \geq 2$ is actually continuous and described by a line of spin-charge separated LL critical points with enhanced symmetry, (ii) the phase transition to the spin-disordered phase is BKT at $\epsilon = 0$, and (iii) the quantum critical point at $\epsilon \neq 0$ occurs at $K_s = 1$, but at strong coupling $\Delta_\epsilon, y \to \infty$. At this fixed point, the spin-charge coupling λ_ϵ, which is relevant (irrelevant) for $K_s > 1$ ($K_s < 1$), becomes marginal. To determine the relevance of λ_ϵ and the nature of the strong coupling phase transition, Eq. (3) is fermionized [47,52] on the $K_s = 1$ hyperplane, leading to $\mathcal{L}_{\text{EP},K_s=1} = \mathcal{L}_{\text{LL}}[\vartheta] + \mathcal{L}_F$

$$\mathcal{L}_F = \frac{1}{2}\eta^T[\partial_\tau + v_s\hat{p}\sigma_z + (M_\epsilon + i\lambda\dot{\vartheta})\sigma_y\kappa_z + M_v\sigma_y]\eta. \quad (5)$$

The Majorana four spinor η is subject to masses $M_\epsilon \sim \Delta_\epsilon\xi_s$, $M_v \sim y\xi_s$ and coupled to the bosonic charge field via $\lambda \sim \lambda_\epsilon\xi_s$. Pauli matrices in left-right (Nambu) space are denoted σ_a (κ_a). At $\lambda = 0$, two Ising transitions occur at $M_\epsilon = \pm M_v$, corresponding to the turquoise disks in Fig. 3(a). The effective theory (5) at the critical point corresponds to a single gapless Majorana mode coupled to a gapless boson by a Lorentz symmetry breaking term. This effective theory is related to the problem studied in Refs. [44–46] by means of a Lorentz boost $(v_s\tau, x) \to (x, -v_s\tau)$ and an analytical continuation $\lambda \to i\lambda$. In that case, an attractive weak coupling fixed point $\lambda \to 0$ with emergent Lorentz symmetry and vanishing velocity $v_c = v_s \to 0$ was uncovered, along with a putative phase separated
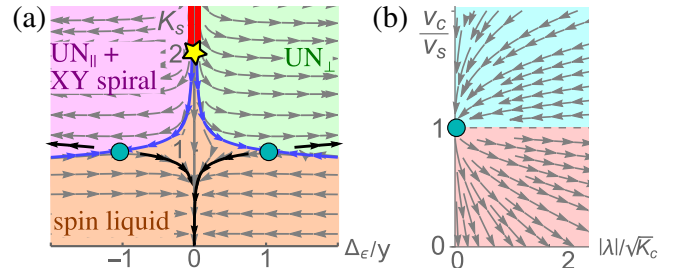

FIG. 3. (a) RG flow according to Eq. (4) in the plane $\Delta_\epsilon y = 0.01$ (color coding as in Fig. 1). The BKT critical end point (Ising fixed point) is represented as a yellow star (turquoise disk). The Ising point resides at $\Delta_\epsilon y = \infty$, and controlled RG equations unveiling its emergent Lorentz symmetry [Eq. (6)], are plotted in (b).

region at strong coupling. Returning to our theory, it is useful to present the one-loop RG equations in terms of $G = |\lambda|/\sqrt{K_c}$, $u = v_c/v_s$, $\bar{v} = \sqrt{v_c v_s}$,

$$\frac{dG}{db} = \frac{uG^3}{8}\frac{(1-u)(3+u)}{(1+u)^2}, \qquad \frac{du}{db} = -\frac{u^2G^2}{4}\frac{(1-u)^2}{(1+u)^2},$$

$$\frac{d\bar{v}}{db} = \frac{u\bar{v}G^2}{8}\frac{10u - u^2 - 1}{(1+u)^2}, \qquad \frac{dK_c}{db} = \frac{uG^2}{4}K_c. \qquad (6)$$

The mass has scaling dimension $1 + uG^2(u + 1/2)/(1 + u)^2$. Because of the imaginary coupling in our model, the flow is reversed as compared to Refs. [44–46]; hence, $\bar{v}$ increases near $u = 1$. The first two RG equations in Eq. (6) decouple and are plotted in Fig. 3(b). The assumption $g_0 > g_2$ implies starting values $v_c > v_s$; therefore, the effective theory (5) resides in the basin of attraction of the weak coupling fixed point $(\lambda, v_c/v_s) = (0, 1)$. By consequence, the critical theory separating the spin disordered from the nematic phases at finite $|\epsilon|$ is a theory with central charge $c = 3/2$, emergent Lorentz symmetry $v_c = v_s$, and logarithmically divergent velocity.

This concludes the derivation of the quantum critical theories. The zero temperature scaling of the order parameter and nematic tensor (Fig. 1) is weakly rounded at finite temperature in the center of a harmonic trapping potential and obtained via a semiclassical evaluation using renormalized coupling constants (see Supplemental Material [47]). In particular, the semiclassically expected first order jump is washed out by the strong quantum fluctuations at $\epsilon = 0$, which corroborates the significance of the quantum field theoretical analysis. It will be interesting to study the predicted QPT numerically using the density matrix renormalization group to solve the SOC spin-1 Bose-Hubbard model [34]. Despite the SOC removing any spin conserving quantum numbers [37], we expect a numerical solution that remains tractable in the superfluid regime, provided that the truncation of the bosonic Hilbert space is treated carefully [38].

[1] H. Ikeda, M.-T. Suzuki, R. Arita, T. Takimoto, T. Shibauchi, and Y. Matsuda, Nat. Phys. **8**, 528 (2012).
[2] A. Koitzsch, N. Heming, M. Knupfer, B. Büchner, P. Y. Portnichenko, A. V. Dukhnenko, N. Y. Shitsevalova, V. B. Filipov, L. L. Lev, V. N. Strocov, J. Ollivier, and D. S. Inosov, Nat. Commun. **7**, 10876 (2016).
[3] V. Martelli, A. Cai, E. Nica, M. Taupin, A. Prokofiev, C.-C. Liu, H.-H. Lai, R. Yu, R. Küchler, A. Strydom, D. Geiger, J. Haenel, J. Larrea, Q. Si, and S. Paschen, arXiv:1709.09376.
[4] Y. Kawaguchi and M. Ueda, Phys. Rep. **520**, 253 (2012).
[5] D. Stamper-Kurn and M. Ueda, Rev. Mod. Phys. **85**, 1191 (2013).
[6] T.-L. Ho, Phys. Rev. Lett. **81**, 742 (1998).
[7] T. Ohmi and K. Machida, J. Phys. Soc. Jpn. **67**, 1822 (1998).
[8] F. Gerbier, A. Widera, S. Fölling, O. Mandel, and I. Bloch, Phys. Rev. A **73**, 041602 (2006).
[9] T. Zibold, V. Corre, C. Frapolli, A. Invernizzi, J. Dalibard, and F. Gerbier, Phys. Rev. A **93**, 023614 (2016).
[10] D. Jacob, L. Shao, V. Corre, T. Zibold, L. De Sarlo, E. Mimoun, J. Dalibard, and F. Gerbier, Phys. Rev. A **86**, 061601 (2012).
[11] C. Frapolli, T. Zibold, A. Invernizzi, K. Jiménez-García, J. Dalibard, and F. Gerbier, Phys. Rev. Lett. **119**, 050404 (2017).
[12] S. Mukerjee, C. Xu, and J. E. Moore, Phys. Rev. Lett. **97**, 120406 (2006).
[13] D. Podolsky, S. Chandrasekharan, and A. Vishwanath, Phys. Rev. B **80**, 214513 (2009).
[14] A. J. A. James and A. Lamacraft, Phys. Rev. Lett. **106**, 140402 (2011).
[15] S. W. Seo, S. Kang, W. J. Kwon, and Y.-i. Shin, Phys. Rev. Lett. **115**, 015301 (2015).
[16] V. M. Galitski and I. Spielman, Nature (London) **494**, 49 (2013).
[17] Y.-J. Lin, R. L. Compton, K. Jimenez-Garcia, J. V. Porto, and I. B. Spielman, Nature (London) **462**, 628 (2009).
[18] Y.-J. Lin, K. Jiménez-García, and I. B. Spielman, Nature (London) **471**, 83 (2011).
[19] B. K. Stuhl, H.-I. Lu, L. M. Aycock, D. Genkina, and I. B. Spielman, Science **349**, 1514 (2015).
[20] D. Campbell, R. Price, A. Putra, A. Valdés-Curiel, D. Trypogeorgos, and I. Spielman, Nat. Commun. **7**, 10897 (2016).
[21] A. Valdés-Curiel, D. Trypogeorgos, E. Marshall, and I. Spielman, New J. Phys. **19**, 033025 (2017).
[22] P. Wang, Z.-Q. Yu, Z. Fu, J. Miao, L. Huang, S. Chai, H. Zhai, and J. Zhang, Phys. Rev. Lett. **109**, 095301 (2012).
[23] L. Huang, Z. Meng, P. Wang, P. Peng, S.-L. Zhang, L. Chen, D. Li, Q. Zhou, and J. Zhang, Nat. Phys. **12**, 540 (2016).
[24] Z. Wu, L. Zhang, W. Sun, X.-T. Xu, B.-Z. Wang, S.-C. Ji, Y. Deng, S. Chen, X.-J. Liu, and J.-W. Pan, Science **354**, 83 (2016).
[25] B. Song, L. Zhang, C. He, T. F. J. Poon, E. Hajiyev, S. Zhang, X.-J. Liu, and G.-B. Jo, Sci. Adv. **4**, eaao4748 (2018).
[26] W. Sun, B.-Z. Wang, X.-T. Xu, C.-R. Yi, L. Zhang, Z. Wu, Y. Deng, X.-J. Liu, S. Chen, and J.-W. Pan, arXiv:1710.00717.
[27] Z. F. Xu, Y. Kawaguchi, L. You, and M. Ueda, Phys. Rev. A **86**, 033628 (2012).
[28] Y. Li, L. P. Pitaevskii, and S. Stringari, Phys. Rev. Lett. **108**, 225301 (2012).
[29] Y. Li, G. I. Martone, L. P. Pitaevskii, and S. Stringari, Phys. Rev. Lett. **110**, 235302 (2013).

[30] C. Hickey and A. Paramekanti, Phys. Rev. Lett. **113,** 265302 (2014).

[31] G. I. Martone, Y. Li, and S. Stringari, Phys. Rev. A **90,** 041604 (2014).

[32] Z. Lan and P. Öhberg, Phys. Rev. A **89,** 023630 (2014).

[33] S. S. Natu, X. Li, and W. S. Cole, Phys. Rev. A **91,** 023608 (2015).

[34] J. H. Pixley, S. S. Natu, I. B. Spielman, and S. Das Sarma, Phys. Rev. B **93,** 081101 (2016).

[35] H. M. Hurst, J. H. Wilson, J. H. Pixley, I. B. Spielman, and S. S. Natu, Phys. Rev. A **94,** 063613 (2016).

[36] G. I. Martone, F. V. Pepe, P. Facchi, S. Pascazio, and S. Stringari, Phys. Rev. Lett. **117,** 125301 (2016).

[37] J. H. Pixley, W. S. Cole, I. B. Spielman, M. Rizzi, and S. Das Sarma, Phys. Rev. A **96,** 043622 (2017).

[38] W. S. Cole, J. Lee, K. W. Mahmud, Y. Alavirad, I. Spielman, and J. D. Sau, arXiv:1711.05794.

[39] Z.-Q. Yu, Phys. Rev. A **93,** 033648 (2016).

[40] K. Sun, C. Qu, Y. Xu, Y. Zhang, and C. Zhang, Phys. Rev. A **93,** 023615 (2016).

[41] F. Zhou, Phys. Rev. Lett. **87,** 080401 (2001).

[42] H. Zhai and F. Zhou, Phys. Rev. B **72,** 014422 (2005).

[43] F. H. L. Essler, G. V. Shlyapnikov, and A. M. Tsvelik, J. Stat. Mech. (**2009**) P02027.

[44] M. Sitte, A. Rosch, J. S. Meyer, K. A. Matveev, and M. Garst, Phys. Rev. Lett. **102,** 176404 (2009).

[45] O. Alberton, J. Ruhman, E. Berg, and E. Altman, Phys. Rev. B **95,** 075132 (2017).

[46] C. L. Kane, A. Stern, and B. I. Halperin, Phys. Rev. X **7,** 031009 (2017).

[47] See Supplemental Material at http://link.aps.org/supplemental/10.1103/PhysRevLett.121.083402 for derivations of the low energy field theory, of RG equations, of the duality transformation, of the scaling of observables and for a discussion of experimental parameters.

[48] G. E. Marti, A. MacRae, R. Olf, S. Lourette, F. Fang, and D. M. Stamper-Kurn, Phys. Rev. Lett. **113,** 155302 (2014).

[49] D. Baillie and P. B. Blakie, Phys. Rev. A **93,** 033607 (2016).

[50] F. Krüger and S. Scheidl, Phys. Rev. Lett. **89,** 095701 (2002).

[51] J. V. José, L. P. Kadanoff, S. Kirkpatrick, and D. R. Nelson, Phys. Rev. B **16,** 1217 (1977).

[52] M. C. Ogilvie, Ann. Phys. (N.Y.) **136,** 273 (1981).